Supporting Information

Understanding Water Adsorption and the Impact on CO_2 Capture in Chemically Stable Covalent Organic Frameworks

Yuxin Ge,[a] Hao Zhou,[a] Yujin Ji,[b] Lifeng Ding,[a] Yuanyuan Cheng,[c] Ruiyao Wang,[a] Siyuan Yang,[a] Yufeng Liu,[a] Xiaoyu Wu,[a] and Youyong Li,*[b]*

a Department of Chemistry, Xi'an JiaoTong-Liverpool University, 111 Ren'ai Road, Suzhou Dushu Lake Higher Education Town, Jiangsu Province, 215123, China

b Institute of Functional Nano & Soft Materials (FUNSOM), Jiangsu Key Laboratory for Carbon-Based Functional Materials & Devices, Soochow University, Suzhou, Jiangsu, 215213, China

c School of Environmental Science & Engineering, Suzhou University of Science & Technology, Suzhou, 215009, China

Yuxin Ge and Hao Zhou contributed equally to this work

Corresponding authors: Lifeng Ding (Lifeng.Ding@xjtlu.edu.cn); Youyong Li (yyli@suda.edu.cn)

Section S-1: Summary of characteristics of the COFs

Table S1. Summary of characteristics of the COFs studied in this work

COFs	V_p, cm^3 g^{-1}		BET	Geometric surface area	Pore Diameter, Å	
	Lit	Sim	m^2 g^{-1}	m^2 g^{-1}	Lit	Sim
COF-42	0.31[1]	1.07	710[5]	2644	23.0[5]	16.47
COF-43	0.36[5]	2.07	620[5]	2571	38.0[5]	31.71
COF-300	0.72[6]	1.19	1360[6]	3453	7.2[6]	8.73
COF-320	0.81[2]	0.60	-	1694	8.0[2]	7.71
COF-LZU1	0.54[7]	1.01	410[7]	2129	12.0[7]	15.15
TpPa-1	-	0.81	535[8]	1639	12.5[8]	15.27
TpPa-2	-	0.63	339[8]	1569	13.5[8]	12.87
TpPa-F4	-	0.51	438[1]	1115	17.0[1]	14.55
TpPa-NO2	-	0.54	129[1]	1254	16.0[1]	
NPN-1	0.48[9]	0.42	-	861	7.3×3.3[9]	3.51, 5.01
NPN-2	0.54[9]	0.46	-	1104	7.8×3.4[9]	3.75, 5.01
NPN-3	0.46[9]	0.34	-	915	5.2×5.2[9]	4.35, 5.25
TpBD	-	1.12	537[10]	1710	17.2[10]	22.11
CTF-1	0.40[11]	0.36	791[11]	905	12.0[11]	8.07
DAAQ-TFP	-	1.10	1280[12]	1737	23.0[12]	21.63

Table S2. Summary of adsorption heats, inflection points and water uptake in p/p_0 = 0.1, 0.3 and 0.9 of the COF at 298 K.

COFs	Adsorption heat	Inflection point	Water uptake, cm^3 g^1		
	kJ mol^{-1}	RH	p/p_0 = 0.1	p/p_0 = 0.3	p/p_0 = 0.9
COF-42	55.89	0.71	326	394	1315
COF-43	65.89	0.78	143	238	2620
COF-300	13.57	0.52	0.049	0.149	0.821
COF-320	29.69	0.52	0.245	0.773	17.267
COF-LZU1	19.79	0.45	0.050	0.164	0.537
TpPa-1	48.17	0.26	65.0	894	962
TpPa-2	58.60	0.26	163	699	747
TpPa-F4	35.11	0.58	0.820	2.474	75.3
TpPa-NO_2	60.47	0.13	410	612	653
NPN-1	24.10	0.45	1.579	207	344
NPN-2	27.73	0.19	18.532	393	435
NPN-3	31.48	0.26	20.286	282	363
TpBD	58.12	0.65	171	196	1347
CTF-1	6.44	0.45	0.005	0.015	28.871
DAAQ-TFP	38.86	0.22	226	1253	1348

Table S3. Summary of the adsorption heats of 6 water models at low coverage in TpPa-1 and TpPa-2.

COFs	TpPa-1	TpPa-2
	Heat of adsorption (kJ mol^{-1})	**Heat of adsorption** (kJ mol^{-1})
SPC	49.00	59.30
SPC/E	48.17	58.60
TIP4P	52.77	61.03
TIP4P_EW	52.79	64.46
TIP5P	39.13	53.49
TIP5P_EW	39.68	52.00

Section S-2: Structure-Property correlations

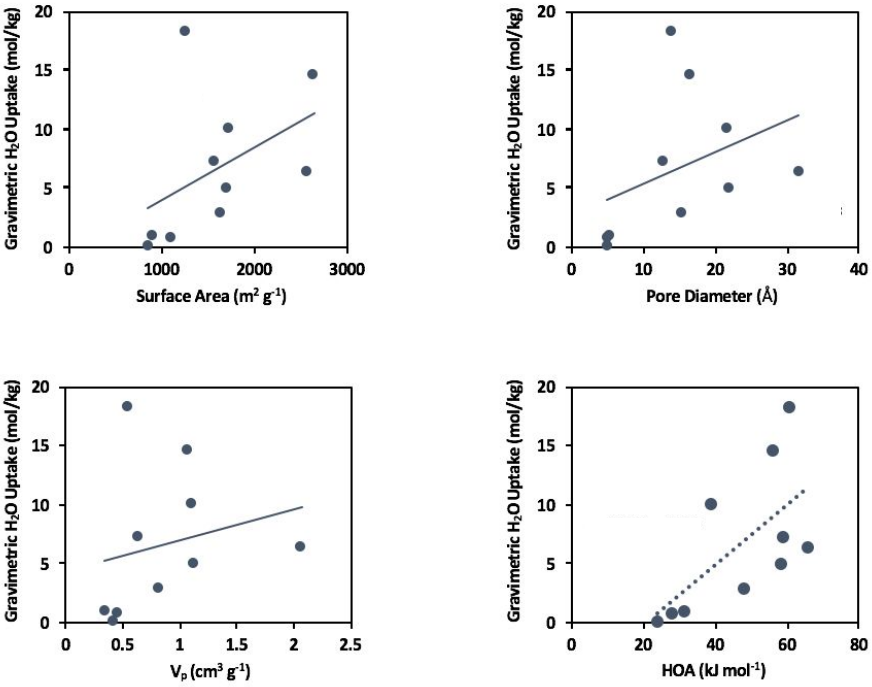

Figure S1. Structure-property correlations between geometric water uptake and the surface area, pore diameter, porosity, heat of adsorption (HOA) of the COFs at RH = 0.1 and 298 K.

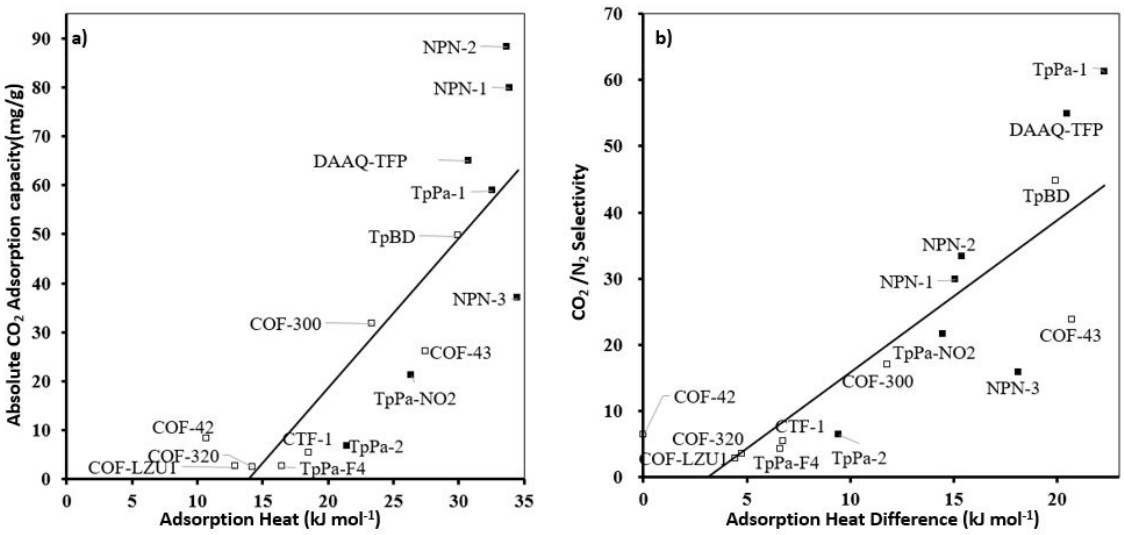

Figure S2. (**a**) Correlation between absolute CO_2 uptake and its isosteric heat of adsorption in the COFs at 1 bar (partial pressure of CO_2 is 0.15 bar, dry condition). (**b**) Correlation between CO_2/N_2 selectivity and the adsorption heat difference of CO_2/N_2 in the COFs at 1 bar (partial pressure of CO_2 is 0.15 bar, dry condition).

Section S-3: Model Clusters and atomic partial charges for TpPa-NO_2

TpPa-NO_2

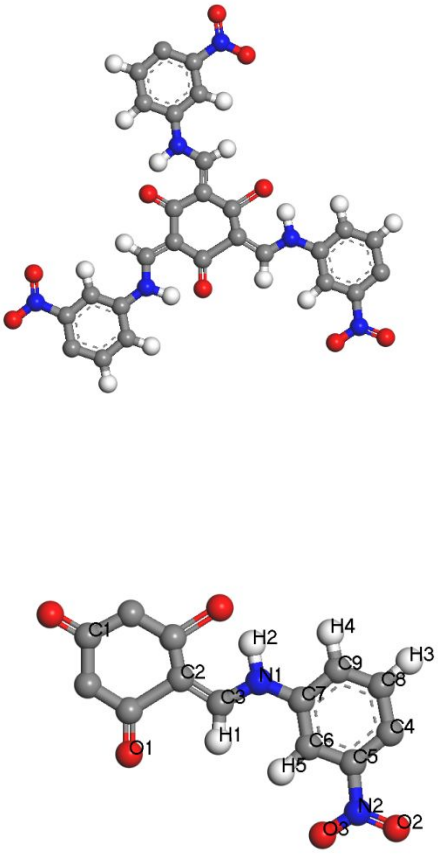

Figure S3. Model cluster used for calculating the partial charges for each atom of TpPa-NO_2.

Table S4. Atomic partial charges calculated using ChelpG method.

Atomic Types	C1	C2	C3	C4	C5	C6	C7	C8	C9	H1
Charge (e)	0.522	-0.347	0.263	0.291	-0.075	-0.260	0.293	-0.209	-0.164	0.071

Atomic Types	H2	H3	H4	H5	N1	N2	O1	O2	O3
Charge (e)	0.371	0.143	0.121	0.171	-0.388	0.721	-0.559	-0.449	-0.449

Section S-4 Simulated water adsorption snapshots in the COFs

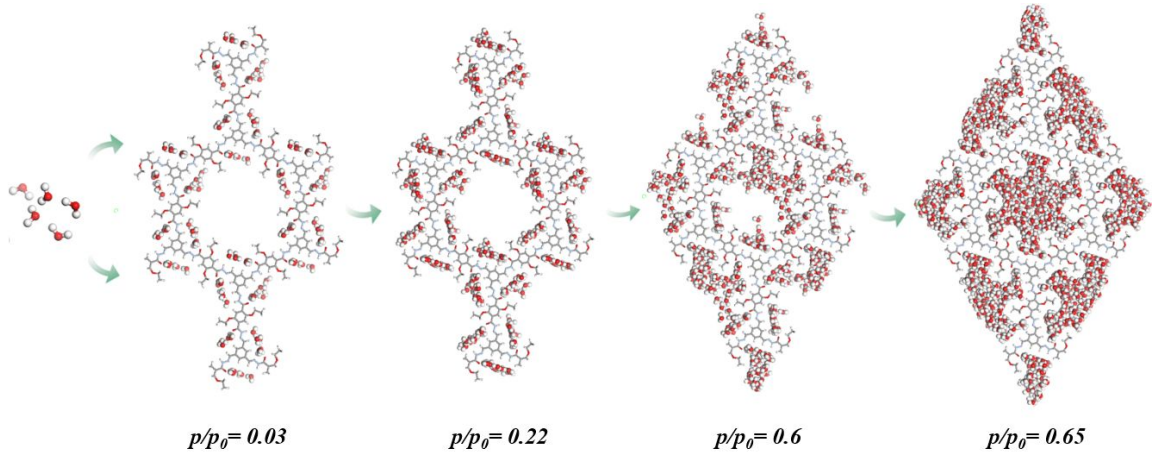

Figure S4. Snapshots of water molecules adsorbed in COF-42 as a function of pressure at 298 K.

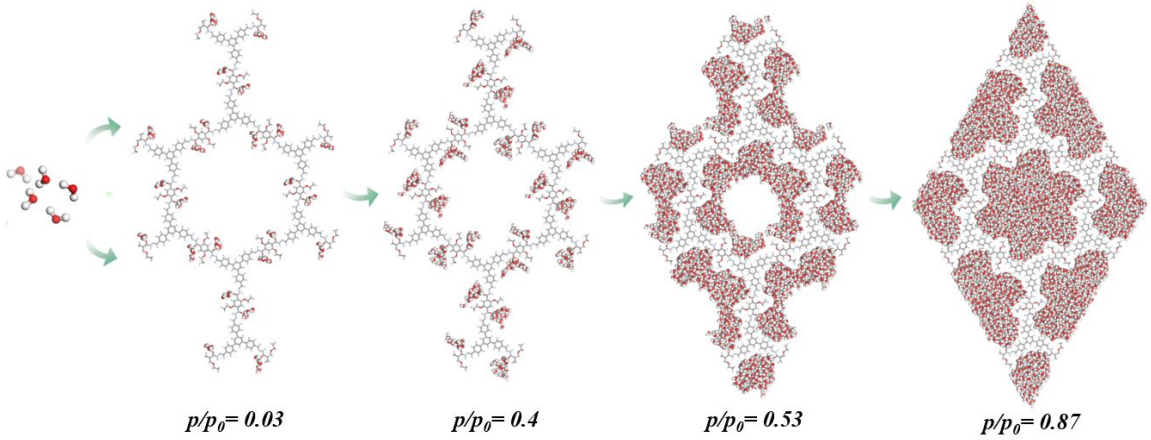

Figure S5. Snapshots of water molecules adsorbed in COF-43 as a function of pressure at 298 K.

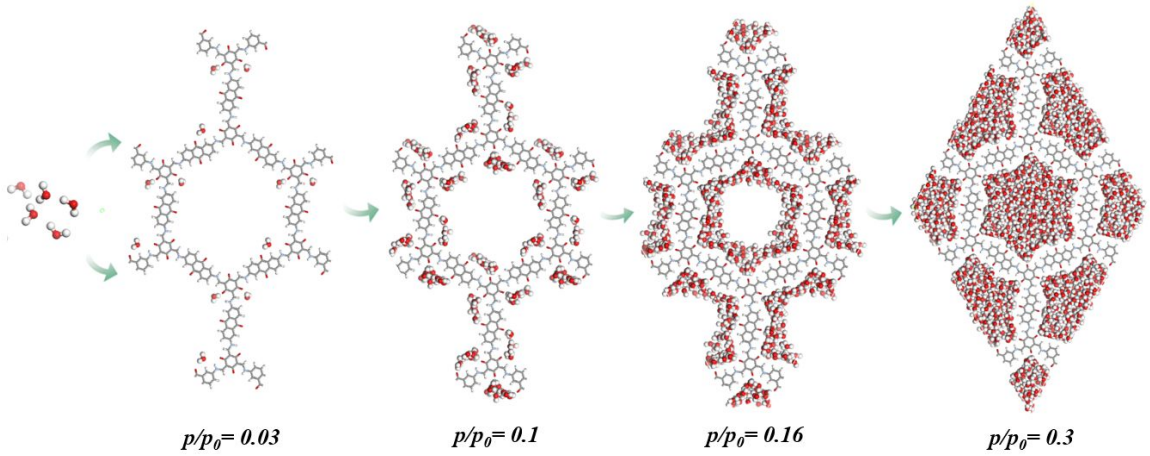

Figure S6. Snapshots of water molecules adsorbed in DAAQ-TFP as a function of pressure at 298 K.

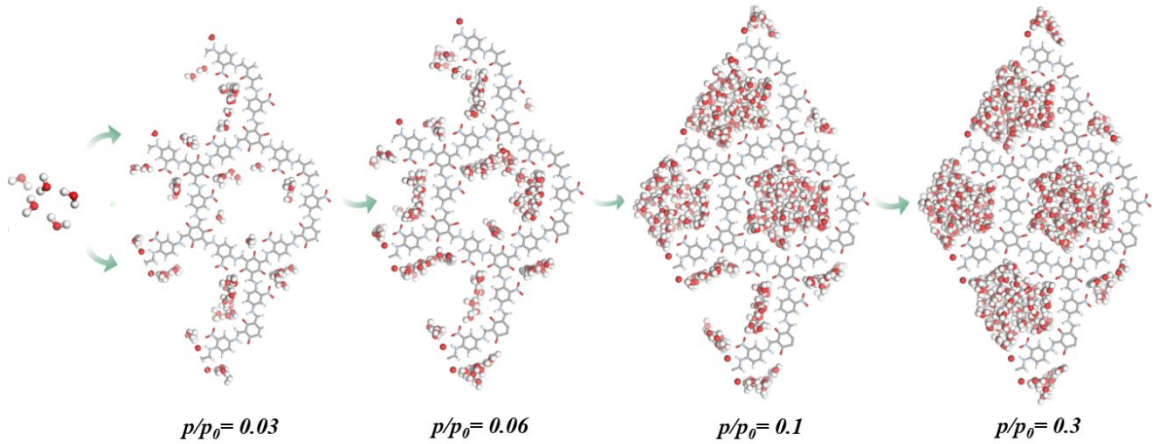

Figure S7. Snapshots of water molecules adsorbed in TpPa-NO_2 as a function of pressure at 298 K.

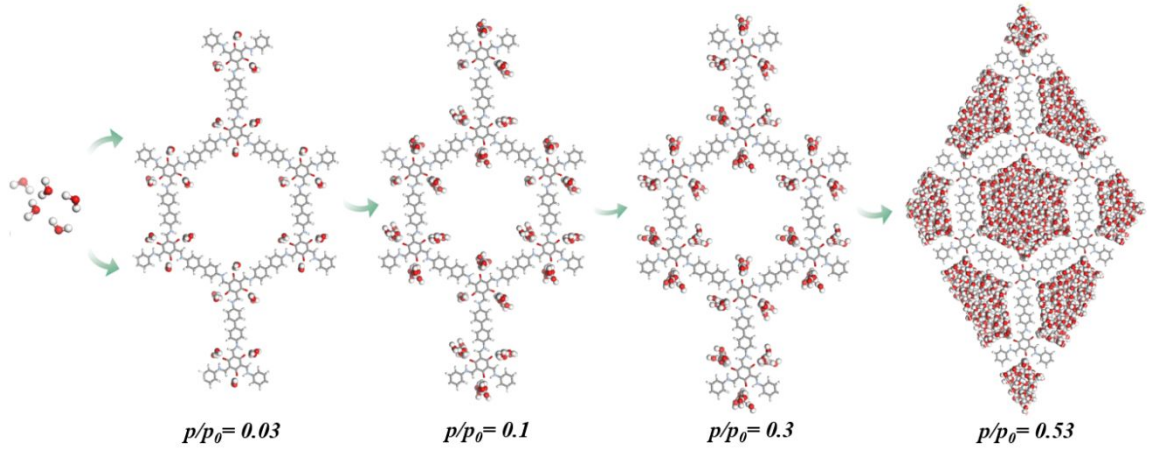

Figure S8. Snapshots of water molecules adsorbed in TpBD as a function of pressure at 298 K.

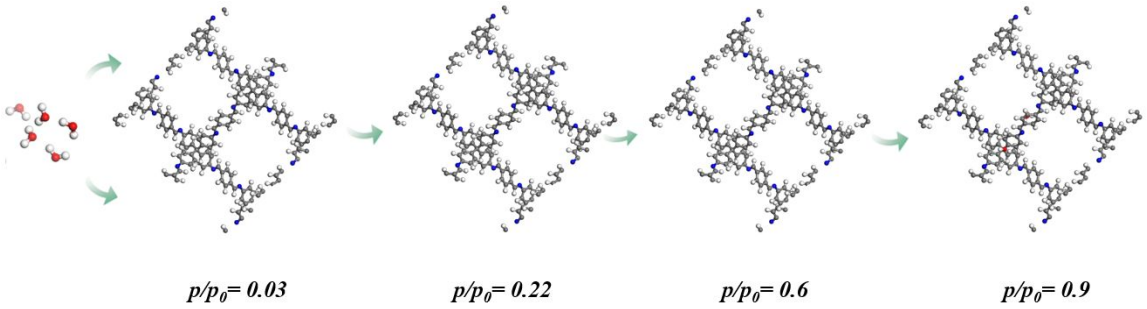

Figure S9. Snapshots of water molecules adsorbed in COF-300 as a function of pressure at 298 K.

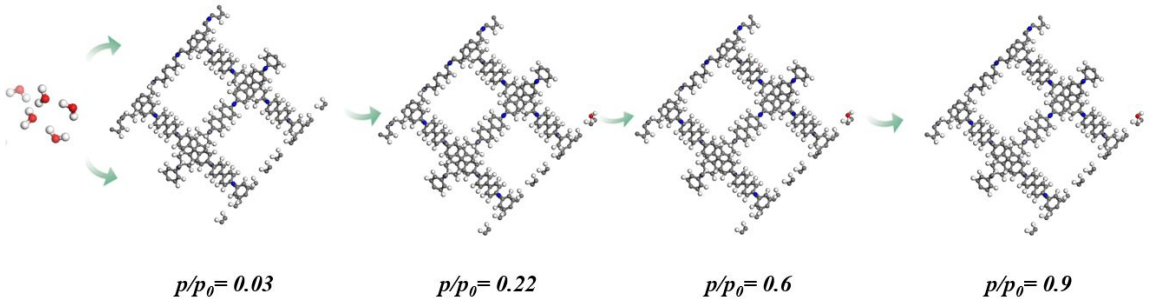

Figure S10. Snapshots of water molecules adsorbed in COF-320 as a function of pressure at 298 K.

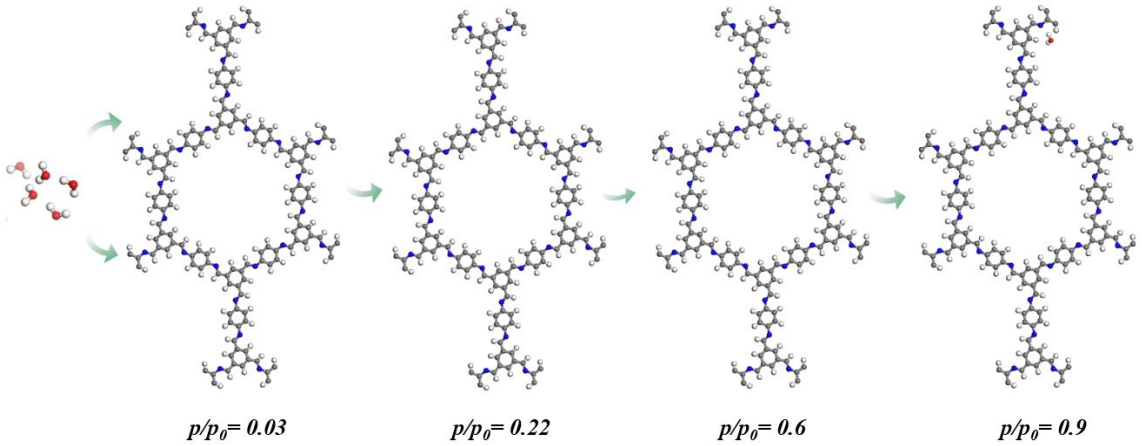

Figure S11. Snapshots of water molecules adsorbed in COF-LZU1 as a function of pressure at 298 K.

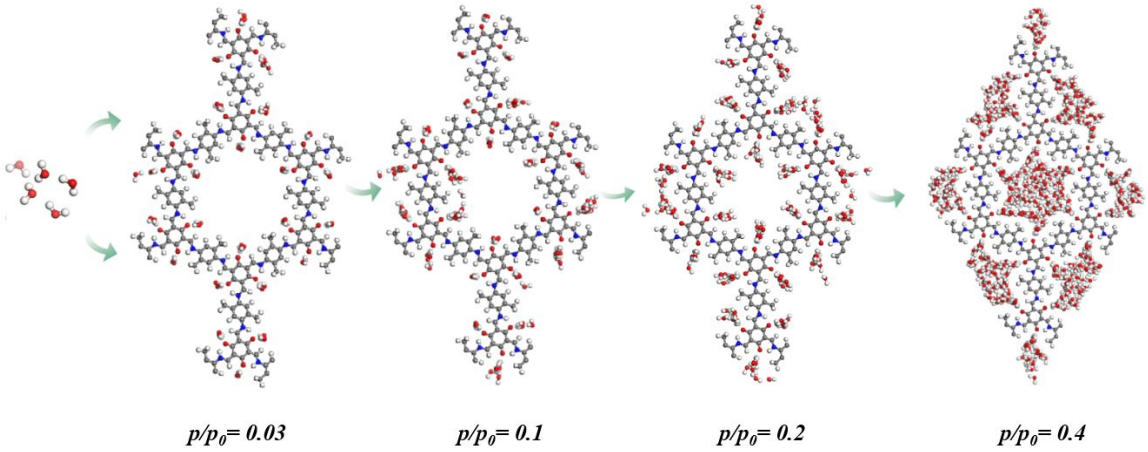

Figure S12. Snapshots of water molecules adsorbed in TpPa-2 as a function of pressure at 298 K.

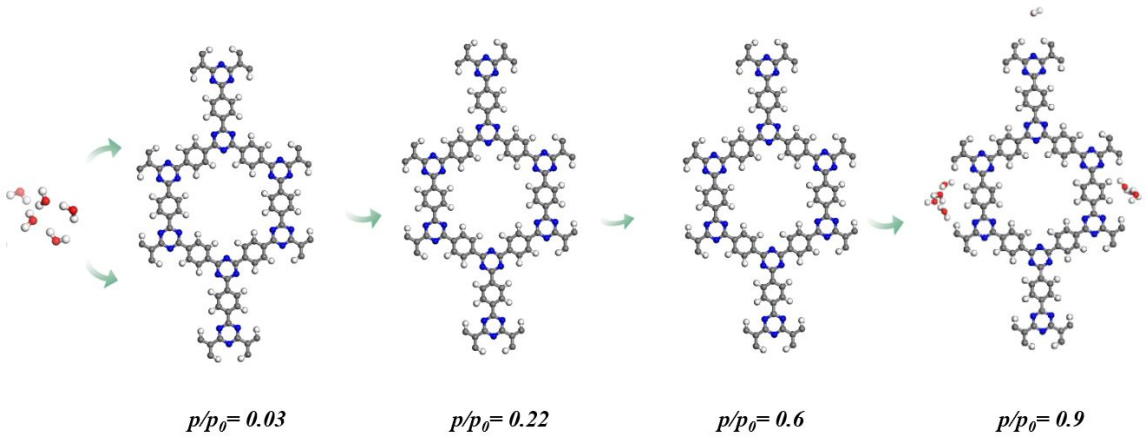

Figure S13. Snapshots of water molecules adsorbed in CTF-1 as a function of pressure at 298 K.

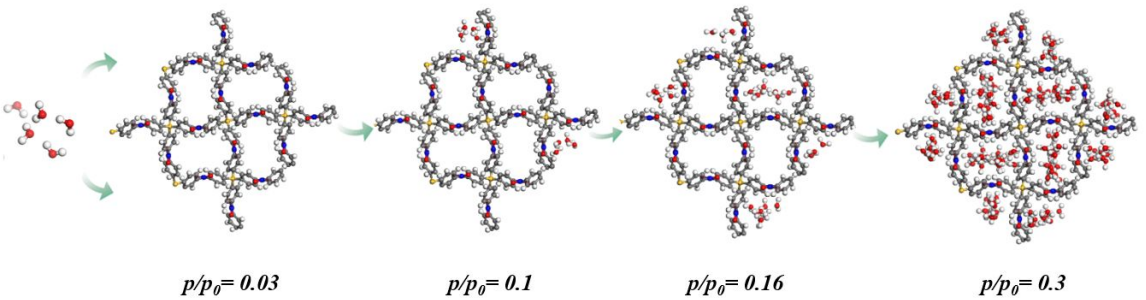

Figure S14. Snapshots of water molecules adsorbed in NPN-2 as a function of pressure at 298 K.

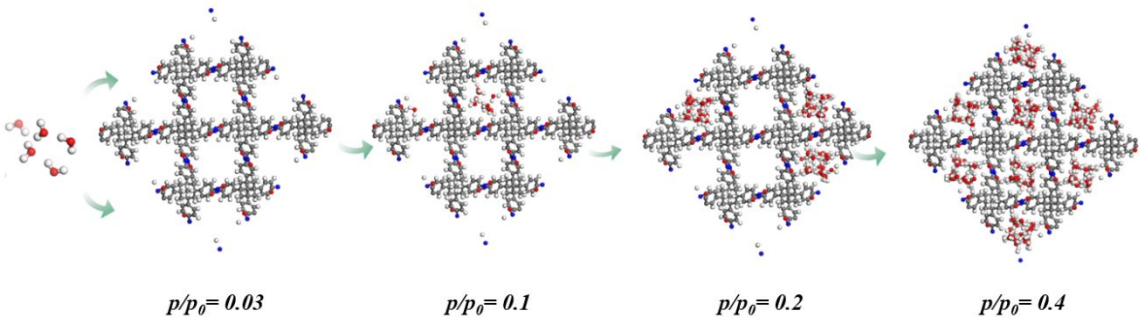

Figure S15. Snapshots of water molecules adsorbed in NPN-3 as a function of pressure at 298 K.

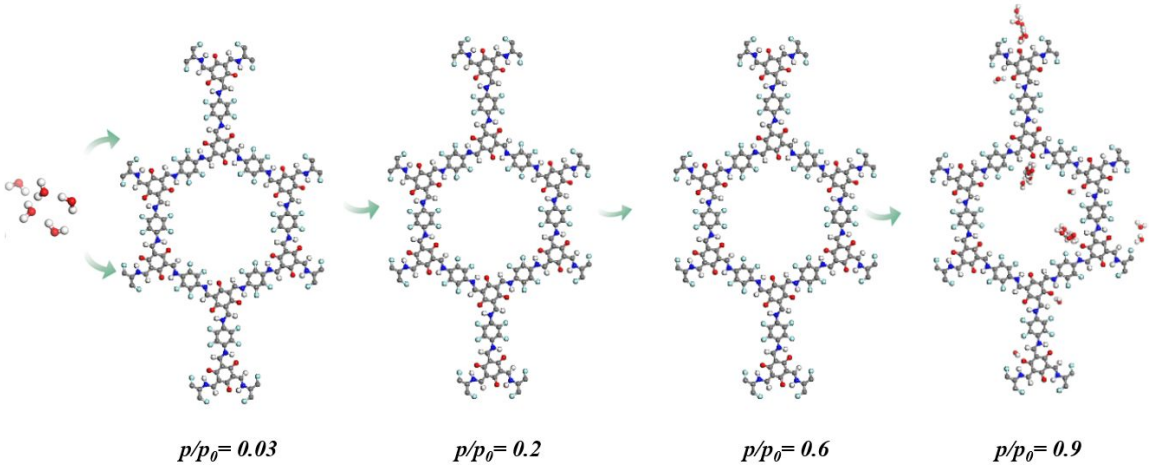

Figure S16. Snapshots of water molecules adsorbed in TpPa-F4 as a function of pressure at 298 K.

Section S-5 Simulated water and CO_2 adsorption density plots in the COFs.

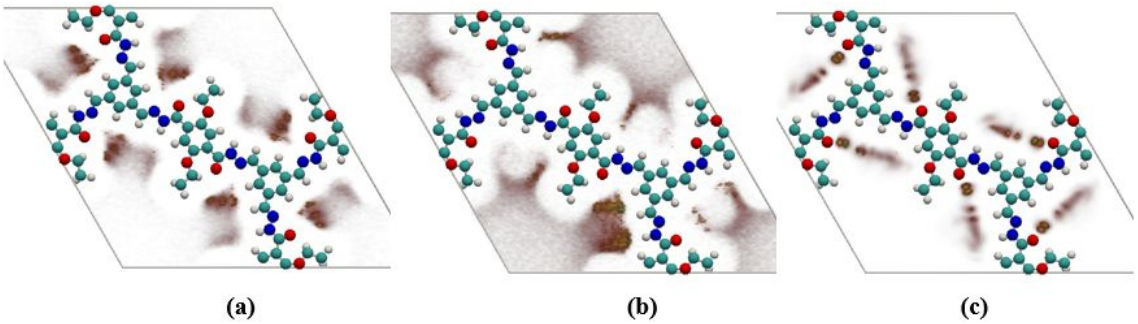

Figure S17. The simulated adsorption density plots of CO_2 **(a)** adsorption in CO_2/N_2 mixture (15:85) with RH = 0, CO_2 **(b)** and water **(c)** adsorption in CO_2/N_2 mixture (15:85) with RH = 0.1 in COF-42 at 298 K and 1 bar. (Color code: N, blue; O, red; C, green; H, white.)

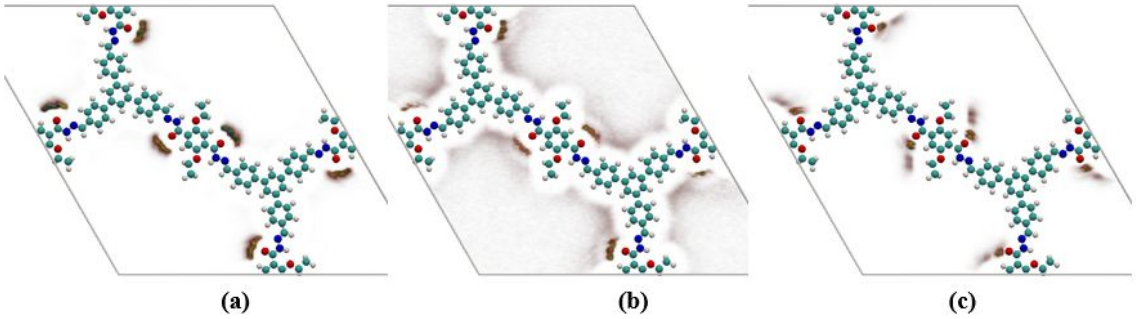

Figure S18. The simulated adsorption density plots of CO_2 **(a)** adsorption in CO_2/N_2 mixture (15:85) with RH = 0, CO_2 **(b)** and water **(c)** adsorption in CO_2/N_2 mixture (15:85) with RH = 0.1 in COF-43 at 298 K and 1 bar. (Color code: N, blue; O, red; C, green; H, white.)

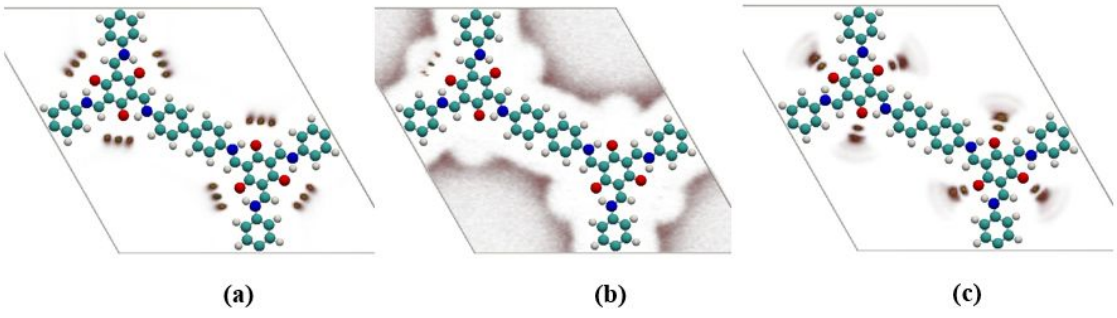

Figure S19. The simulated adsorption density plots of CO_2 (**a**) adsorption in CO_2/N_2 mixture (15:85) with RH = 0, CO_2 (**b**) and water (**c**) adsorption in CO_2/N_2 mixture (15:85) with RH = 0.1 in TpBD at 298 K and 1 bar. (Color code: N, blue; O, red; C, green; H, white.)

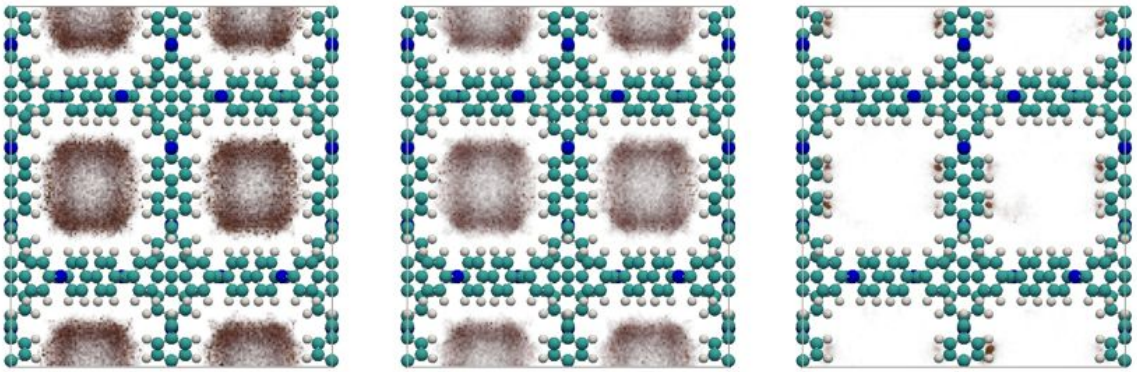

Figure S20. The simulated adsorption density plots of CO_2 **(a)** adsorption in CO_2/N_2 mixture (15:85) with RH = 0, CO_2 **(b)** and water **(c)** adsorption in CO_2/N_2 mixture (15:85) with RH = 0.1 in COF-320 at 298 K and 1 bar. (Color code: N, blue; O, red; C, green; H, white.)

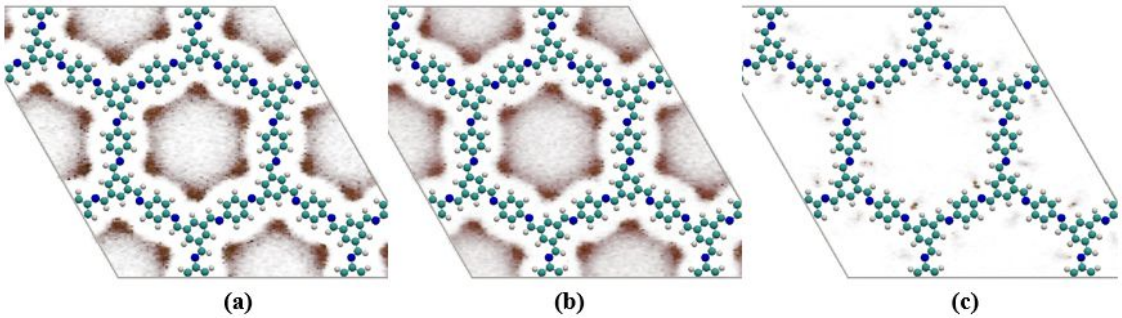

Figure S21. The simulated adsorption density plots of CO_2 **(a)** adsorption in CO_2/N_2 mixture (15:85) with RH = 0, CO_2 **(b)** and water **(c)** adsorption in CO_2/N_2 mixture (15:85) with RH = 0.1 in COF-LZU1 at 298 K and 1 bar. (Color code: N, blue; O, red; C, green; H, white.)

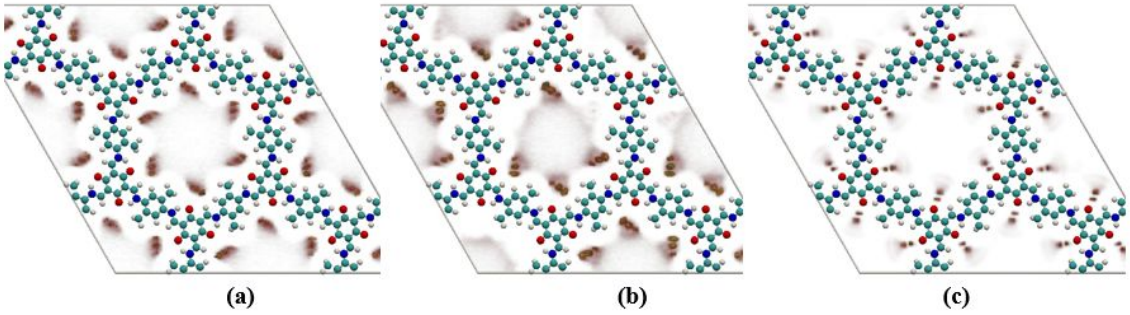

Figure S22. The simulated adsorption density plots of CO_2 **(a)** adsorption in CO_2/N_2 mixture (15:85) with RH = 0, CO_2 **(b)** and water **(c)** adsorption in CO_2/N_2 mixture (15:85) with RH = 0.1 in TpPa-2 at 298 K and 1 bar. (Color code: N, blue; O, red; C, green; H, white.)

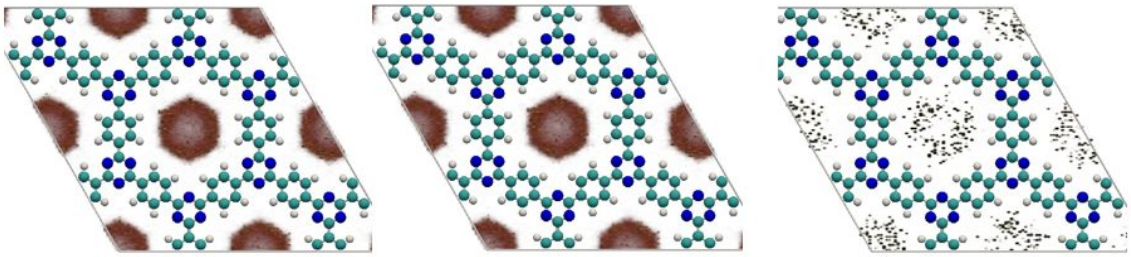

(a) (b) (c)

Figure S23. The simulated adsorption density plots of CO_2 **(a)** adsorption in CO_2/N_2 mixture (15:85) with RH = 0, CO_2 **(b)** and water **(c)** adsorption in CO_2/N_2 mixture (15:85) with RH = 0.1 in CTF-1 at 298 K and 1 bar. (Color code: N, blue; O, red; C, green; H, white.)

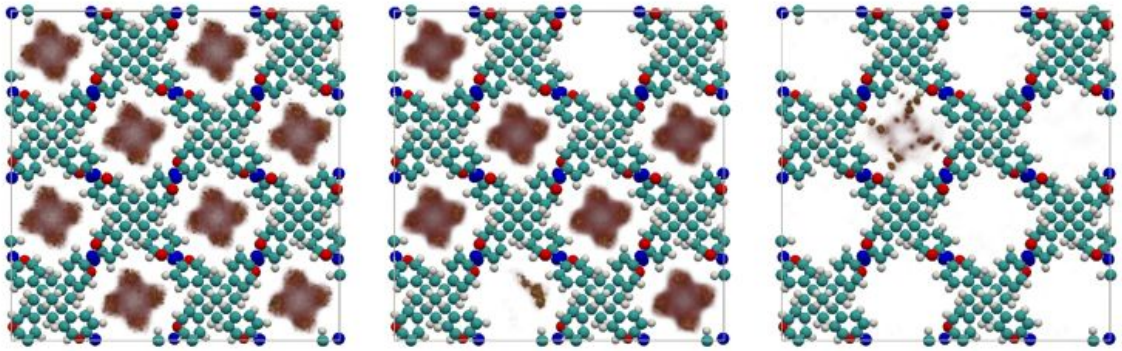

(a) (b) (c)

Figure S24. The simulated adsorption density plots of CO_2 **(a)** adsorption in CO_2/N_2 mixture (15:85) with RH = 0, CO_2 **(b)** and water **(c)** adsorption in CO_2/N_2 mixture (15:85) with RH = 0.1 in NPN-3 at 298 K and 1 bar. (Color code: N, blue; O, red; C, green; H, white.)

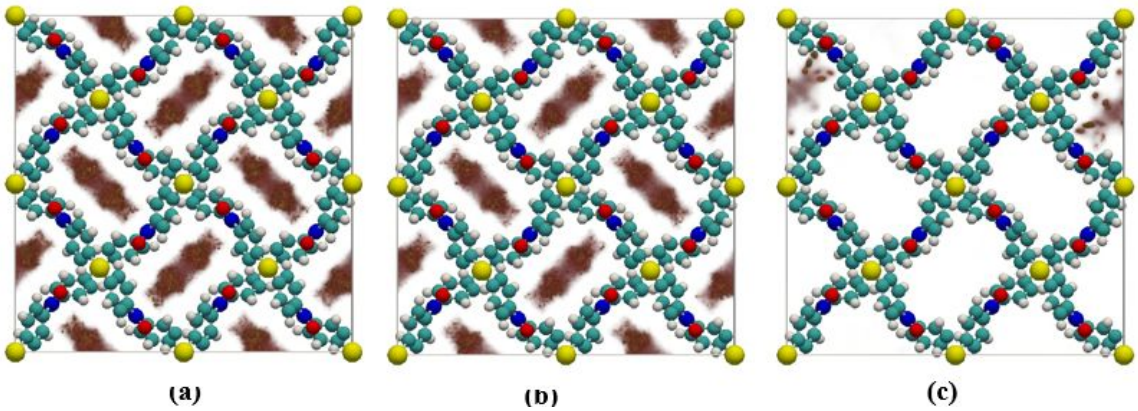

(a) (b) (c)

Figure S25. The simulated adsorption density plots of CO_2 **(a)** adsorption in CO_2/N_2 mixture (15:85) with RH = 0, CO_2 **(b)** and water **(c)** adsorption in CO_2/N_2 mixture (15:85) with RH = 0.1 in NPN-2 at 298 K and 1 bar. (Color code: N, blue; O, red; C, green; H, white.)

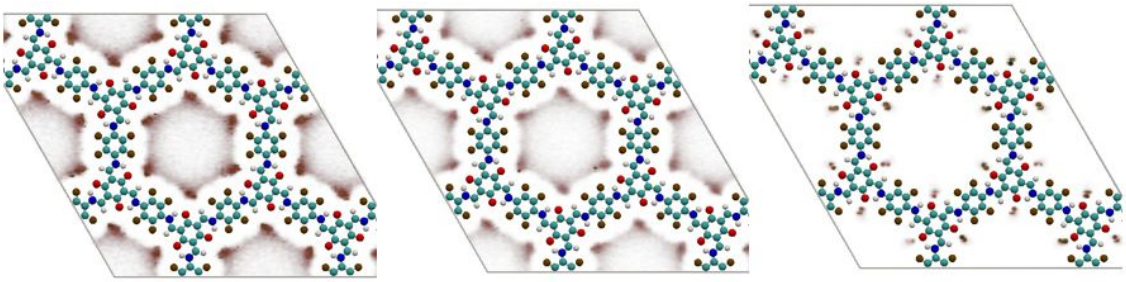

(a) (b) (c)

Figure S26. The simulated adsorption density plots of CO_2 **(a)** adsorption in CO_2/N_2 mixture (15:85) with RH = 0, CO_2 **(b)** and water **(c)** adsorption in CO_2/N_2 mixture (15:85) with RH = 0.1 in TpPa-F4 at 298 K and 1 bar. (Color code: N, blue; O, red; C, green; H, white.)

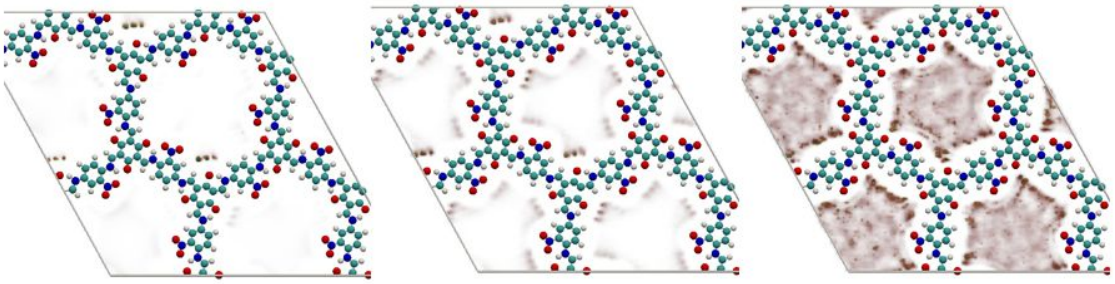

(a) (b) (c)

Figure S27. The simulated adsorption density plots of CO_2 **(a)** adsorption in CO_2/N_2 mixture (15:85) with RH = 0, CO_2 **(b)** and water **(c)** adsorption in CO_2/N_2 mixture (15:85) with RH = 0.1 in TpPa-NO_2 at 298 K and 1 bar. (Color code: N, blue; O, red; C, green; H, white.)

Section S-6 Pore Size Distributions of the COFs

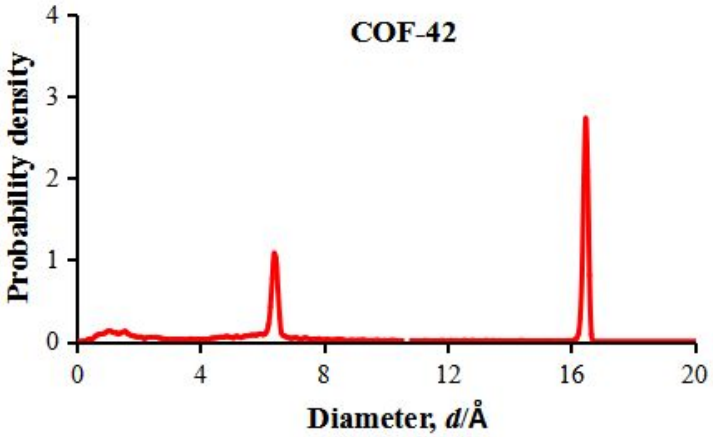

Figure S28. Pore Size distribution for COF-42.

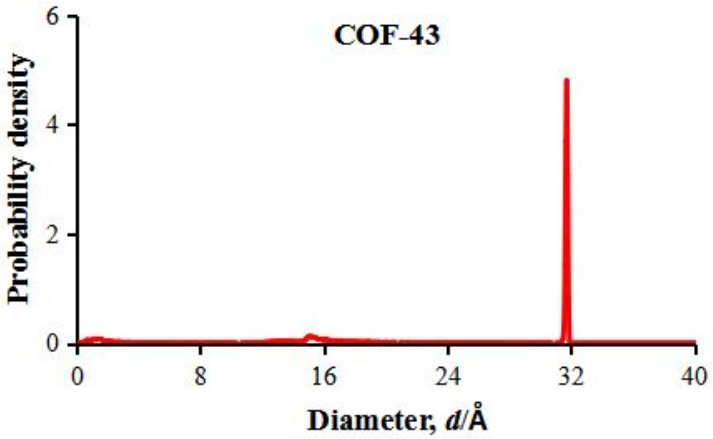

Figure S29. Pore Size distribution for COF-43.

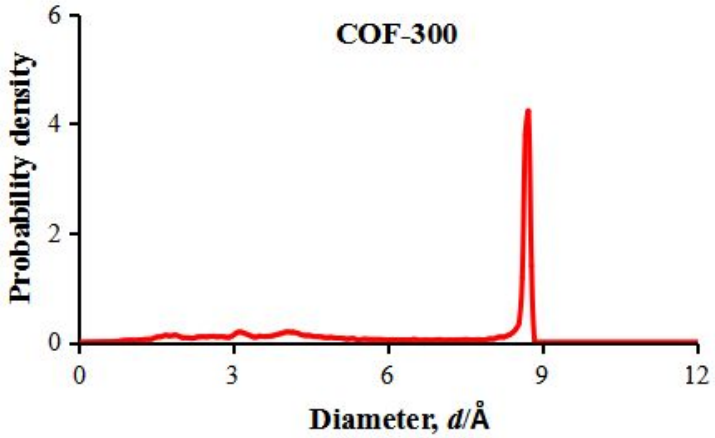

Figure S30. Pore Size distribution for COF-300.

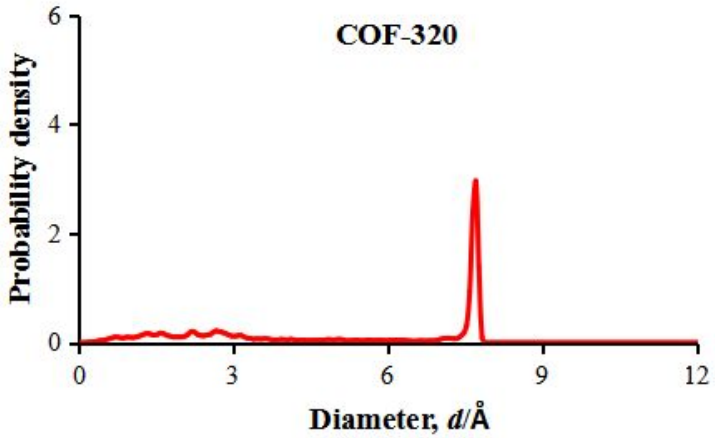

Figure S31. Pore Size distribution for COF-320.

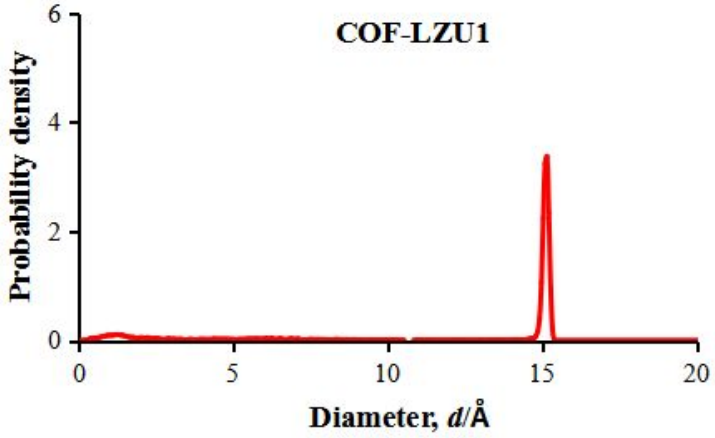

Figure S32. Pore Size distribution for COF-LZU1.

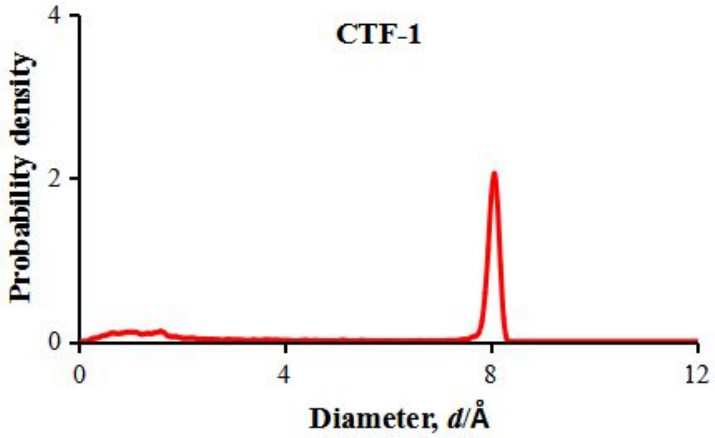

Figure S33. Pore Size distribution for CTF-1.

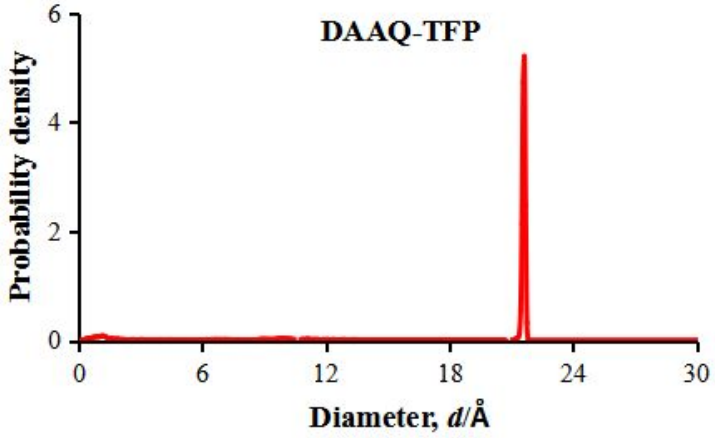

Figure S34. Pore Size distribution for DAAQ-TFP.

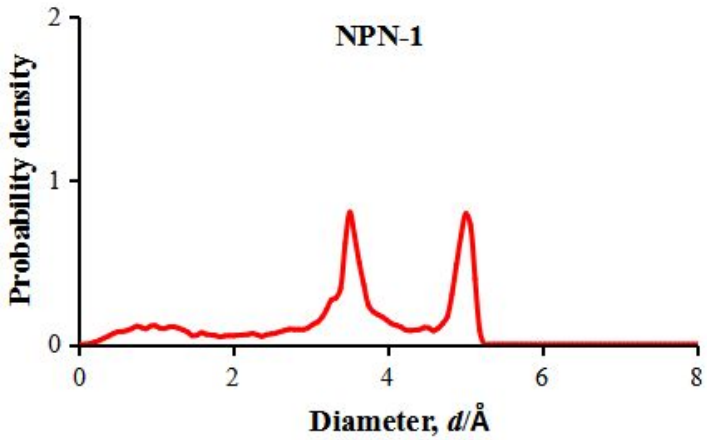

Figure S35. Pore Size distribution for NPN-1.

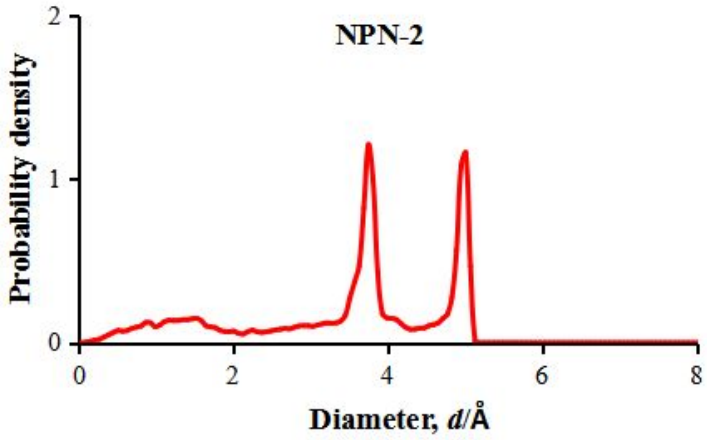

Figure S36. Pore Size distribution for NPN-2.

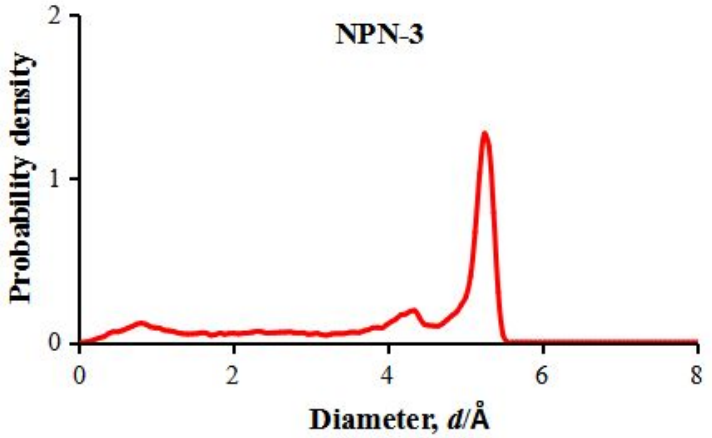

Figure S37. Pore Size distribution for NPN-3.

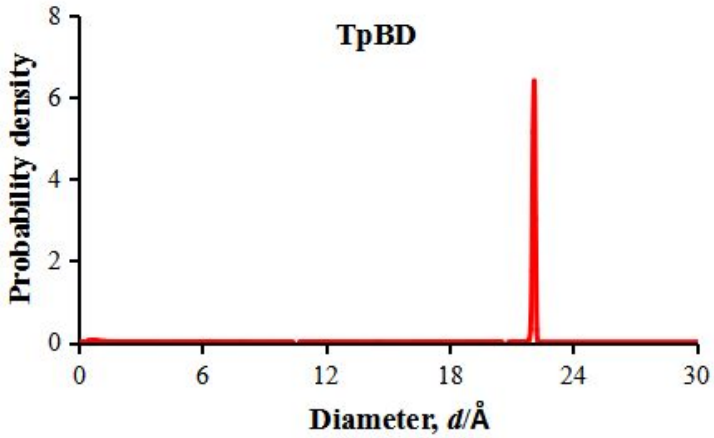

Figure S38. Pore Size distribution for TpBD.

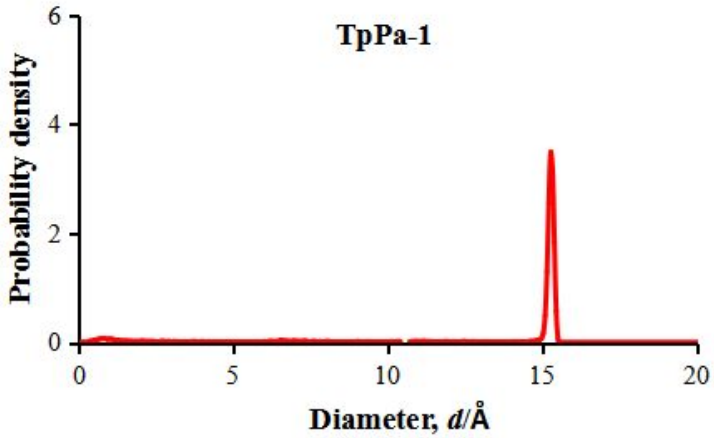

Figure S39. Pore Size distribution for TpPa-1.

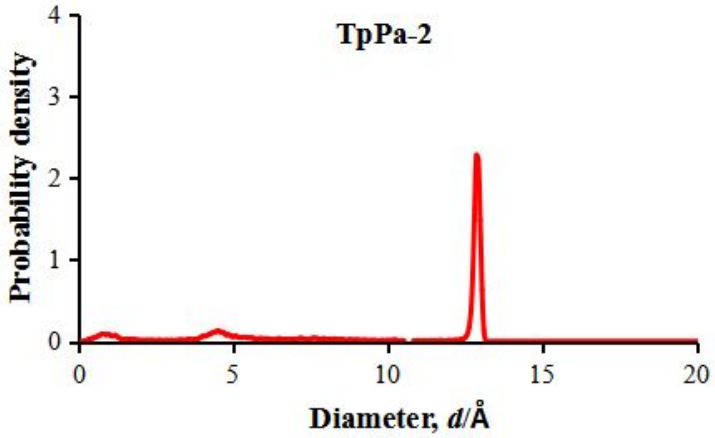

Figure S40. Pore Size distribution for TpPa-2.

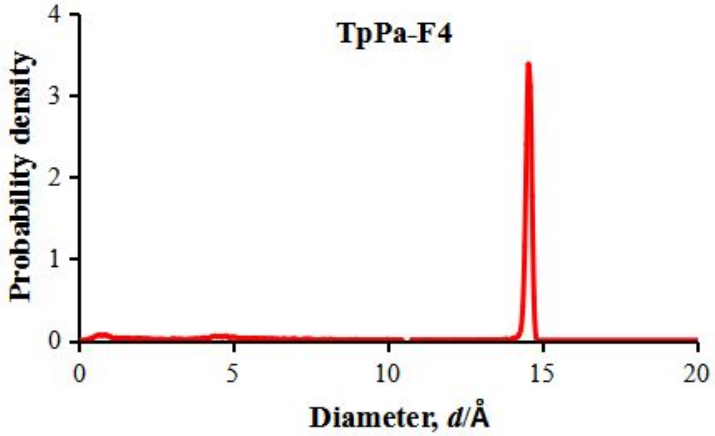

Figure S41. Pore Size distribution for TpPa-F4.

Section S-7 Radial distribution functions (RDF) of the oxygen-oxygen distance between oxygen atoms of the water molecules and the COF framework oxygen atoms

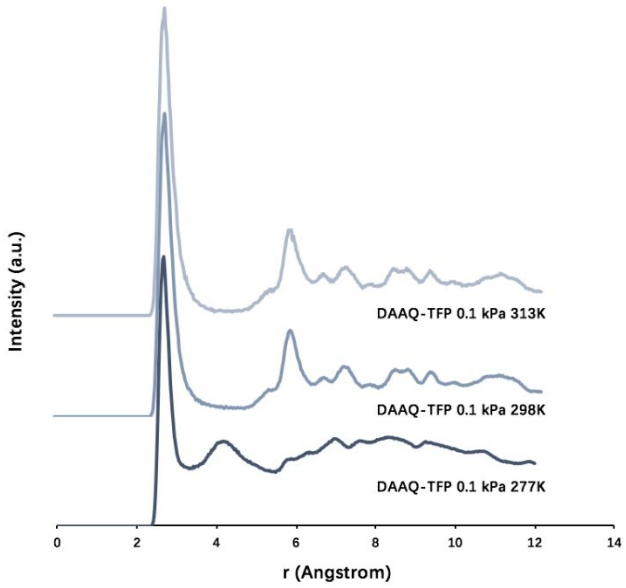

Figure S42. Radial distribution function (RDF) of the oxygen-oxygen distance between oxygen atom of the adsorbed water molecules and the COF framework oxygen atoms in DAAQ-TFP at different temperatures and 0.1 kPa.

Section S-8 Force field parameters used in the GCMC simulations

Table S5. Lennard-Jones parameters for the framework atoms of the COFs.

Atoms	C	O	H	N	F	Si
σ(Å)	3.47	3.03	2.85	3.26	3.09	3.80
ε/k_B	47.86	48.16	7.650	38.95	156.0	10.53

ε is the well depth, σ is the diameter. The LJ interaction parameters are from DREIDING force field.

Table S6. Force-Field parameters and geometries of six water models considered in this study

Model	**Sites**	σ (Å)	ι_1 (Å)	ι_2 (Å)	q_1 (e)	q_2 (e)	θ (^{O})	φ(^{O})
SPC	Three	3.1656	1.000	-	+0.4100	-0.8200	109.47	-
SPC/E	Three	3.1656	1.000	-	+0.4238	-0.8476	109.47	-
TIP4P	Four	3.1540	0.957	0.150	+0.5200	-1.0400	104.52	52.26
TIP4P_Ew	Four	3.1643	0.957	0.125	+0.5242	-1.0484	104.52	52.26
TIP5P	Five	3.1200	0.957	0.700	+0.2410	-0.2410	104.52	109.47
TIP5P_Ew	Five	3.0970	0.957	0.700	+0.2410	-0.2410	104.52	109.47

References

(1) Chandra, S.; Kandambeth, S.; Biswal, B. P.; Lukose, B.; Kunjir, S. M.; Chaudhary, M.; Babarao, R.; Heine, T.; Banerjee, R. Chemically Stable Multilayered Covalent Organic Nanosheets from Covalent Organic Frameworks via Mechanical Delamination. *J. Am. Chem. Soc.* **2013**, 135, 17853-17861.

(2) Zhang, Y.; Su, J.; Furukawa, H.; Yun, Y.; Gá, F. Single-Crystal Structure of a Covalent Organic Framework. *J. Am. Chem. Soc.* **2013**, 7–10.

(3) Furukawa, H.; Yaghi, O. M. Storage of Hydrogen, Methane, and Carbon Dioxide in Highly Porous Covalent Organic Frameworks for Clean Energy Applications. *J. Am. Chem. Soc.* **2009**, 131, 8875-8883.

(4) Nagai, A.; Guo, Z.; Feng, X.; Jin, S.; Chen, X.; Ding, X.; Jiang, D. Pore Surface Engineering in Covalent Organic Frameworks. *Nat. Commun.* **2011**, 2, 536.

(5) Uribe-Romo, F. J.; Doonan, C. J.; Furukawa, H.; Oisaki, K.; Yaghi, O. M. Crystalline Covalent Organic Frameworks with Hydrazone Linkages: Journal of the American Chemical Society. *J. Am. Chem. Soc.* **2011**, *133*, 11478–11481.

(6) Uribe-romo, F. J.; Hunt, J. R.; Furukawa, H.; Klo, C.; Keeffe, M. O.; Yaghi, O. M. Communication A Crystalline Imine-Linked 3-D Porous Covalent Organic Framework A Crystalline Imine-Linked 3-D Porous Covalent Organic Framework. *J. Am. Chem. Soc.* **2009**, 131, 4570–4571.

(7) Ding, S.-Y.; Gao, J.; Wang, Q.; Zhang, Y.; Song, W.-G.; Su, C.-Y.; Wang, W. Construction of Covalent Organic Framework for Catalysis: Pd/COF-LZU1 in Suzuki-Miyaura Coupling Reaction. *J. Am. Chem. Soc.* **2011**, *133*, 19816–19822.

(8) Kandambeth, S.; Mallick, A.; Lukose, B.; Mane, M. V.; Heine, T.; Banerjee, R. Construction of Crystalline 2D Covalent Organic Frameworks with Remarkable Chemical (Acid/Base) Stability via a Combined Reversible and Irreversible Route. *J. Am. Chem. Soc.* **2012**, *134*, 19524–19527.

(9) Tong, M.; Yang, Q.; Zhong, C. Computational Screening of Covalent Organic Frameworks for CH4/H2, CO2/H2 and CO2/CH4 Separations. *Microporous Mesoporous Mater.* **2015**, *210*, 142–148.

(10) Biswal, B. P.; Chandra, S.; Kandambeth, S.; Lukose, B.; Heine, T.; Banerjee, R. Mechanochemical

Synthesis of Chemically Stable Isoreticular Covalent Organic Frameworks. *J. Am. Chem. Soc.* **2013**, *135*, 5328–5331.

(11) Kuhn, P.; Antonietti, M.; Thomas, A. Porous, Covalent Triazine-Based Frameworks Prepared by Ionothermal Synthesis. *Angew. Chemie Int. Ed.* **2008**, *47*, 3450–3453.

(12) DeBlase, C. R.; Silberstein, K. E.; Truong, T.T.; Abruña, H. D.; Dichtel, W. R. β-Ketoenamine-Linked Covalent Organic Frameworks Capable of Pseudocapacitive Energy Storage. *J. Am. Chem. Soc.* **2013**, *135*, 16821–16824.

(13) Tong, M.; Yang, Q.; Xiao, Y.; Zhong, C. Revealing the Structure-Property Relationship of Covalent Organic Frameworks for CO_2 Capture from Postcombustion Gas: A Multi-Scale Computational Study. *Phys. Chem. Chem. Phys.* **2014**, 16, 15189-15198.